Metabolic Changes Induced by the Biliopancreatic Diversion in Diet-Induced Obesity in Male Rats: The Contributions of Sleeve Gastrectomy and Duodenal Switch

Elena-Dana Baraboi,* Wei Li,* Sébastien M. Labbé, Marie-Claude Roy, Pierre Samson, Frédéric-Simon Hould, Stéphane Lebel, Simon Marceau, Laurent Biertho, and Denis Richard

Institut Universitaire de Cardiologie et de Pneumologie de Québec, Chemin Sainte-Foy, Québec, Canada G1V 4G5

The mechanisms underlying the body weight and fat loss after the biliopancreatic diversion with duodenal switch (BPD/DS) remain to be fully delineated. The aim of this study was to examine the contributions of the two main components of BPD/DS, namely sleeve gastrectomy (SG) and duodenal switch (DS), on energy balance changes in rats rendered obese with a high-fat (HF) diet. Three different bariatric procedures (BPD/DS, SG, and DS) and three sham surgeries were performed in male Wistar rats. Sham-operated animals fed HF were either fed ad libitum (Sham HF) or pair weighed (Sham HF PW) by food restriction to the BPD/DS rats. A group of sham-operated rats was kept on standard chow and served as normal diet control (Sham Chow). All three bariatric surgeries resulted in a transient reduction in food intake. SG per se induced a delay in body weight gain. BPD/DS and DS led to a noticeable gut malabsorption and a reduction in body weight and fat gains along with significant elevations in plasma levels of glucagon-like peptide-1_{7-36} and peptide YY. BPD/DS and DS elevated energy expenditure above that of Sham HF PW during the dark phase. However, they reduced the volume, oxidative metabolism, and expression of thermogenic genes in interscapular brown adipose tissue. Altogether the results of this study suggest that the DS component of the BPD/DS, which led to a reduction in digestible energy intake while sustaining energy expenditure, plays a key role in the improvement in the metabolic profile led by BPD/DS in rats fed a HF diet. (***Endocrinology*** **156: 1316–1329, 2015)**

The biliopancreatic diversion (BPD) with duodenal switch (DS) is one of the most successful bariatric procedures to treat severe obesity and to resolve type 2 diabetes. Long-term clinical studies have reported remarkable reductions in the percentage of excess weight after BPD/DS (1, 2). This surgery leads to substantial metabolic improvements including normalization of plasma glucose, insulin, triglycerides, and free fatty acids (1, 3). Compared with other bariatric procedures such as sleeve gastrectomy (SG) alone or Roux-en-Y intestinal gastric bypass (RYGB), BPD/DS is performed much less frequently (4). It, however, still remains a highly effective surgery, presenting metabolic benefits, which are more persistent than those of other bariatric procedures (5). Recent meta-analyses revealed that BPD/DS achieved greater weight loss and a higher dia-

ISSN Print 0013-7227 ISSN Online 1945-7170
Printed in U.S.A.

Received September 24, 2014. Accepted January 10, 2015.
First Published Online February 3, 2015

* E.-D.B. and W.L. contributed equally to this work.

Abbreviations: BAT, brown adipose tissue; BPD, biliopancreatic diversion; COX4, cytochrome c oxidase subunit IV; CPT1, carnitine palmitoyl transferase I; CT, computed tomography; DS, duodenal switch; EDL, extensor digitorum longus; FM, fat mass; ^{18}FTHA, 14-R,S-18F-fluoro-6-thiaheptadecanoic acid; GI, gastrointestinal; GIP, gastric inhibitory peptide; HF, high fat; iBAT, interscapular BAT; GLP-1, glucagon-like peptide-1; NEFA, nonesterified fatty acid; PET, positron emission tomography; PGC1, peroxisome proliferator-activated receptor-γ coactivator 1; PW, pair weighed; PYY, peptide YY; RM-ANOVA, repeated-measures ANOVA; ROI, region of interest; RQ, respiratory quotient; RYGB, Roux-en-Y intestinal gastric bypass; SG, sleeve gastrectomy; UCP1, uncoupling protein 1; VO_2, oxygen consumption; WAT, white adipose tissue.

betes remission rate than RYGB, SG, and adjustable gastric banding (6, 7).

The mechanisms whereby BPD/DS induces long-lasting metabolic benefits are partially understood. The BPD/DS developed by Marceau et al (3, 8) basically consists of the association of vertical SG with DS. SG reduces the gastric reservoir capacity, whereas the DS reengineers the intestine to divert the biliopancreatic secretion to the distal ileum and creates a shorter passage of the nutriments in the intestinal tract. As a consequence, the distal gut becomes the main site for nutrient absorption. Our animal model of BPD/DS reproduces the BPD/DS surgery that we perform in humans (9, 10). We previously demonstrated that the BPD/DS in chow-fed rats induced a marked reduction in body weight and fat mass gain and resulted in a negative energy balance compared with a sham operation (9, 10). These effects were persistent up to 2 months after the surgery (9, 10).

The recent human and animal studies that have attempted to elucidate the mechanisms behind the metabolic benefits of bariatric surgery have mainly focused on RYGB and SG. Initially it was suggested that mechanical restriction and nutrient malabsorption were responsible for weight loss after bariatric surgery (11, 12). However, the most recent literature suggests that additional mechanisms contribute to the body weight loss after SG and RYGB. No consensus exists regarding the changes in energy expenditure after bariatric procedures. Studies performed in humans and rodents have shown either increases (13–16) or decreases (17–19) in energy expenditure after RYGB. More consistent evidence exists regarding the effects of bariatric surgeries on the eating behavior and gut function. RYGB and SG reduce food intake while increasing preference for diets of low caloric density (20, 21), accelerating gastric emptying (22, 23) and enhancing nutrient delivery in the contact of the enteroendocrine cells in the distal gut (24, 25). RYGB and SG have also been associated with high postprandial plasma levels of glucagon-like peptide 1 (GLP-1) and peptide YY (PYY) (26–28), which may play a role in the improving of glucose tolerance and the resolution of type 2 diabetes (29, 30). Recent studies brought new hypothesis about the role of bile acids and fibroblast growth factor-19 as well as gut microbiota on incretin secretion after RYGB (31) and SG (32).

The main objective of the present study was to delineate the contributions of SG and DS to the metabolic improvements produced by the BPD/DS in rats fed a high-fat (HF) diet to induce obesity. Energy balance measurements were carried out in BPD/DS, DS, SG, and sham-operated rats over 9 weeks after the surgery. Changes in plasma levels of gastrointestinal (GI) hormones were evaluated at the end of the experimental period. The thermogenic activity of the interscapular brown adipose tissue (iBAT) was estimated using the positron emission tomography (PET) tracers ^{11}C-acetate (oxidative activity) and 14-R,S-18F-fluoro-6-thiaheptadecanoic acid (^{18}FTHA-free fatty acid uptake). We also assessed the expression of genes encoding proteins involved in brown adipose tissue (BAT) thermogenesis and fatty acid oxidation.

Materials and Methods

Animals and diets

Animal care and handling were performed in accordance with the Canadian Guide for the Care and Use of Laboratory Animals, and all experimental procedures received approval of the Laval University Animal Care Committee and the Animal Ethics Committee of the University of Sherbrooke (for the imaging study).

Male Wistar rats initially weighing between 250 and 275g were purchased from Charles River Canada and were individually housed in plastic cages under controlled conditions (ambient temperature, 23°C ± 1°C; 12 h light, 12 h dark cycle, lights on 6:00 AM to 6:00 PM). For 6 weeks before surgery, rats were fed a HF diet (D12492; Research Diets) or standard chow (2018 formula, Teklad diets; Harlan Laboratories). Details regarding the energy content of the diets are provided in the Supplemental Materials and Methods.

The HF-fed rats were randomly assigned to four types of surgery (BPD/DS, SG, DS, and sham surgery). These groups presented comparable body weights on the day of their surgery. On day 8 after surgery, HF-fed, sham-operated animals were further randomly divided into two groups: ad libitum fed rats (Sham HF) and food restricted, sham-operated rats [Sham HF pair weighed (PW)]. Starting on day 9, Sham HF PW rats were allowed to eat a restricted amount of food to maintain a body weight comparable with that of BPD/DS rats. The amount of food in Sham HF PW rats was readjusted every day, and it was offered in two meals (one third of the amount was given in the morning and the remaining two thirds were offered at dark onset), this to minimize the meal-feeding effects. A chow-fed group was sham operated, and it was used as a diet-control group (Sham Chow) to demonstrate the obesity-inducing effect of HF feeding.

Bariatric surgery procedures

All rats were operated under isoflurane anesthesia. BPD/DS was performed as previously described (10) (Supplemental Figure 1). After a 3-cm midline laparotomy, the small intestine was exposed and transected at 50 cm above the ileocecal junction. The proximal part of the cut intestine was then end-to-side anastomosed to the distal part of the intestine (ileum) at 20 cm from the ileocecal junction to create a 20-cm common limb, which receives largely undigested nutrients together with the biliopancreatic juice. We then anastomosed the distal part of the cut intestine to the duodenum at 1–1.5 cm from the pylorus to form the alimentary limb. The duodenum was then ligated between the duodenal anastomosis and the biliopancreatic duct to separate the biliopancreatic limb and ensure the channeling of food only into the alimentary limb. Lengths of 50 and 20 cm were used for the alimentary and common limbs to keep the proportions

used in human BPD/DS surgery (33). A gastric sleeve was achieved by excising the aglandular forestomach, estimated to be two-thirds of the gastric capacity in the rat. A double suture was performed to obtain a leak-proof tubular stomach.

SG rats were subjected to the SG procedure solely, whereas the DS rats were assigned to the gut-reengineering procedure only (Supplemental Figure 1). The sham surgery consisted in a midline laparotomy, the handling of the intestines and stomach, and the suture of the abdominal wall. The sham surgery was kept simple to reduce the time of operation. However, we demonstrated in a series of experiments that this sham surgery produced effects on the growth curve in the rat similar to those seen using a more elaborated sham procedure involving sham gastrectomy with suture and intestinal anastomoses (Supplemental Figure 2). Further details regarding the surgery and cares associated with it are found in the Supplemental Materials and Methods.

Only the rats that did not present any sign of postoperative complications and that did stay in good health were included in the statistical analyses. In BPD/DS and DS rats, the duodenal closure was carefully verified at the time the animals were killed, and only animals maintaining intact closure (integrity of the suture and absence of the food in biliopancreatic limb) were included in the analyses. Rats who died or were killed because of postsurgical complications were excluded from the study. Eighty percent of deaths were registered during the first 2 postoperative days, whereas the other 20% were registered during the first 2 weeks. We operated with an overall success rate of 68.5%. Forty-eight rats were used for the metabolic assessments: BPD/DS (n = 11), SG (n = 8), DS (n = 7), Sham HF fed ad libitum (n = 6), Sham HF PW (pair weighted with BPD/DS) (n = 8), and Sham Chow (n = 8). Additional groups of rats were used for the imaging study: BPD/DS (n = 7), SG (n = 6), DS (n = 5), Sham HF (n = 6), Sham HF PW (n = 6), and Sham Chow (n = 6).

Body weight and body composition

Rats were weighted daily throughout the 9-week experimental period. On day 3 before surgery and on postoperative day 49, all rats had their body composition estimated by whole-body computed tomography (CT) scans (eXplore CT 120 Micro CT; GE Healthcare Pre-Clinical) performed under isoflurane anesthesia. Clavicles (rostrally) and the fifth caudal vertebra (caudally) were used as anatomical reference points to demarcate the scanned area used for the body composition analysis. The percentage of body fat was measured and the fat mass (FM) was calculated. The fat-free mass was calculated by subtraction of FM from total body weight.

Energy intake

Food and water intake were measured daily throughout the experimental period. Food spillage was carefully collected and accounted for in the intake measurements. Fecal energy loss was evaluated before and after surgery. Feces were collected over a 24-hour period on day −3 (prior to surgery) and on postoperative days 28 and 59. After collection, feces were dried and weighed and their energy content was measured by bomb calorimetry (Parr 6100 calorimeter). The gross energy content of the diet was also assessed by bomb calorimetry. Digestible energy intake was calculated as the gross energy intake minus the fecal energy content. Energy digestibility (percentage) was computed as the ratio of digestible energy intake to gross energy intake. During the sixth week after surgery, rats were subjected to a meal test to evaluate the effects of the surgery on food intake during a restricted amount of time. Rats were then allowed to eat freely for 1 hour after an overnight fast and the amount of food consumed during the hour was measured.

Indirect calorimetry and locomotor activity

During the postoperative week 8, energy expenditure was measured using indirect calorimetry. Locomotor activity was also monitored. Rats were individually housed in metabolic chambers, under the same light and temperature conditions as described above. Water and food were available ad libitum. The metabolic chambers (AccuScan Instruments) consisted of rectangular, air-proof cages (30 × 30 × 20 cm) linked to an open-circuit flow-through calorimetric device connected to a computer-controlled system of data acquisition. A grid of infrared light beams detected the animal's position 16 times per second and allowed monitoring of locomotor activity. Rats were housed into the metabolic cages 24 hours prior to measurement to accustom them to their new environment. Oxygen consumption (VO_2) and carbon dioxide production were recorded every 15 minutes over 24 hours. Hourly averages of values of VO_2 and hourly sums of distance traveled (locomotor activity) were calculated and used into the statistical analyses. The respiratory quotient (the carbon dioxide production to VO_2 ratio) was also calculated.

Tissue sampling

At the end of the ninth postoperative week, after an overnight fast, all rats were given ketamine (60 mg/kg)/xylazine (7.5 mg/kg) ip. Rats were then intracardially perfused with ice-cold isotonic saline. The gut, pancreas, liver, heart, soleus and extensor digitorum longus (EDL) muscles, iBAT, inguinal, retroperitoneal and epididymal white adipose tissues (WAT) were quickly dissected out and weighed. iBAT samples were quickly frozen in liquid nitrogen and stored at −80°C, pending gene expression measurements. In the BPD/DS- and DS-operated rats, specimens of the alimentary, biliopancreatic, and common limbs were taken from the proximal portion of each limb. In the sham- and SG-operated rats, gut samples were obtained from corresponding levels of intestine. Gut specimens were cleaned in ice-cold saline and then fixed in a sodium phosphate-buffered paraformaldehyde solution (4%) at 4°C for 1–2 weeks prior to being embedded in paraffin. The gut segments were then cut into 5-μm transversal slices and mounted on slides for hematoxylin and eosin staining to examine the histological structures and perform morphological measurements.

Plasma variables

Plasma levels of the GI hormones, GLP-1_{7-36}, PYY, ghrelin, and gastric inhibitory peptide (GIP), as well as insulin, C-peptide, leptin, and plasma metabolites (glucose, triglycerides, nonesterified fatty acid (NEFA), and cholesterol) were measured on week 9. At the time the animals were killed (from 9:00 to 11:00 AM), after an overnight fast, blood was collected by cardiac puncture using syringes containing EDTA 0.5 M. Further information on blood processing and a description of the kits used for measuring different plasma parameters are provided in the Supplemental Materials and Methods.

BAT gene expression

iBAT mRNAs coding for uncoupling protein 1 (UCP1) and for cytochrome c oxidase subunit IV (COX4), carnitine palmitoyl transferase I (CPT1), and peroxisome proliferator-activated receptor-γ coactivator 1α (PGC1α) were quantified using real-time PCR analyses. Acidic ribosomal protein L27 was used as reference gene as no significant difference in its expression was observed between various groups. Target gene mRNA expression was evaluated as the ratio of amount of target template to reference template. Details are provided in the Supplemental Materials and Methods.

iBAT metabolism and free fatty acid uptake

Experiments were performed in 12-hour-fasted rats anesthetized with 1.5% (vol/vol) isoflurane (Abbott Laboratories) delivered through a nose cone with an oxygen rate set at 0.75 L/min. A catheter was placed into tail vein for iv infusions of the PET tracers. The experiments were initiated 15 minutes after insertion of the catheter.

Imaging experiments were performed with the Triumph dual-modality PET/CT scanner having an 8-cm axial FOV (Gamma Medica) at the Sherbrooke Molecular Imaging Centre (Sherbrooke, Canada). During imaging protocols, rats rested supine on the scanner bed and were kept warm with a heating pad. Boluses of each radiopharmaceutical (17–20 Mbq in 0.5 mL of 0.9% NaCl) were injected via the caudal vein over 30 seconds. A 20-minute dynamic acquisition with ^{11}C-acetate was done to determine tissue oxidative metabolism. Ten minutes after the first scan, a 30-minute dynamic acquisition with ^{18}FTHA was done to determine the active iBAT volume based on fatty acid uptake, as previously described (34, 35). After the PET procedure, a CT scan was acquired with the detector-source assembly rotating over 360° and 720 rotation steps image dynamic data analysis was performed as described previously (34, 36, 37). The iBAT was visualized on three-dimensional CT-PET coregistration images with the Amide software (version 1.0.5, amide.sourceforge.net). To measure the volume of activated iBAT, a region of interest (ROI) contour was delineated based on a threshold equal to the maximum ^{18}FTHA activity minus 1 SD of all voxels within the primary visually defined ROI. The volume of the newly ROI was used to report the active iBAT volume within the fat content delineated by the CT images.

Statistical analysis

Results were expressed as mean values ± SEM. Comparisons between groups were analyzed using a one-way ANOVA followed by Bonferoni's multiple comparison tests or least significance difference tests among preplanned comparisons (six of 15 comparisons). Between-group differences in the VO_2, respiratory quotient (RQ), and locomotor activity over the respective experimental periods were determined by repeated-measures ANOVA (RM-ANOVA) using a mixed-model ANOVA followed by Bonferoni's multiple comparison tests. Differences were considered as being significant when the value was $P < .05$. Statistical analyses were performed with GraphPad Prism version 6 (GraphPad Software).

Results

Body weight and body composition

Bariatric surgery had marked effects on body weight of rats (Figure 1A and Table 1). During the first 2 weeks after the surgery, SG, DS, and BPD/DS rats gained significantly less weight than sham rats fed ad libitum (Figure 1A). In the BPD/DS and DS rats, but not in SG rats, the reducing effect on body weight persisted until the end of the experimental period (Figure 1A and Table 1). At the end of the study, the final body weight and total body weight gain were markedly lower in BPD/DS and DS rats compared with Sham HF and expectedly similar to that of Sham HF PW animals (Figure 1B and Table 1). A trend toward a reduced total body weight gain was observed in SG animals over the 9-week experimental period ($P = .08$ vs Sham HF, Figure 1B). The complete time course of body weight is indicated in Supplemental Figure 3.

Together with affecting weight gain, bariatric surgery also influenced body composition as evaluated with CT. BPD/DS and DS, but not SG, significantly reduced the fat mass gain (Figure 1C). At the time of death, weight of adipose tissue was lower in BPD/DS and DS rats than in the Sham HF group (Table 1). The reducing effect of BPD/DS and DS surgeries was seen in all adipose tissue depots. BPD/DS and DS surgeries also reduced EDL muscle mass, and lower liver and heart weights were observed at the time the animals were killed in the BPD/DS, DS, and Sham HF PW animals compared with the Sham HF rats. In contrast, a higher pancreas weight was seen in BPD/DS and DS rats compared with the Sham HF and Sham HF PW animals (Table 1).

Energy intake

Bariatric surgery transiently lowered food intake (Figure 1D). During the first 2 postoperative weeks, all three groups of operated rats (eg, SG, DS, and BPD/DS) showed a gross energy intake significantly lower than that of Sham HF animals. During the following weeks, SG, DS, and BPD/DS rats progressively increased their food intake. Thus, during the second part of the protocol, all groups fed ad libitum showed similar levels of gross energy intake. Because Sham HF PW animals were food restricted, their cumulative energy intake was significantly lower than that of the other groups throughout the whole experimental period ($P < .001$ vs Sham HF and $P < .05$ vs BPD/DS). The complete time course of body weight is indicated in Supplemental Figure 3.

BPD/DS and DS surgeries resulted in energy malabsorption (Figure 2). Higher fecal energy density content was recorded in BPD/DS and DS rats as compared with

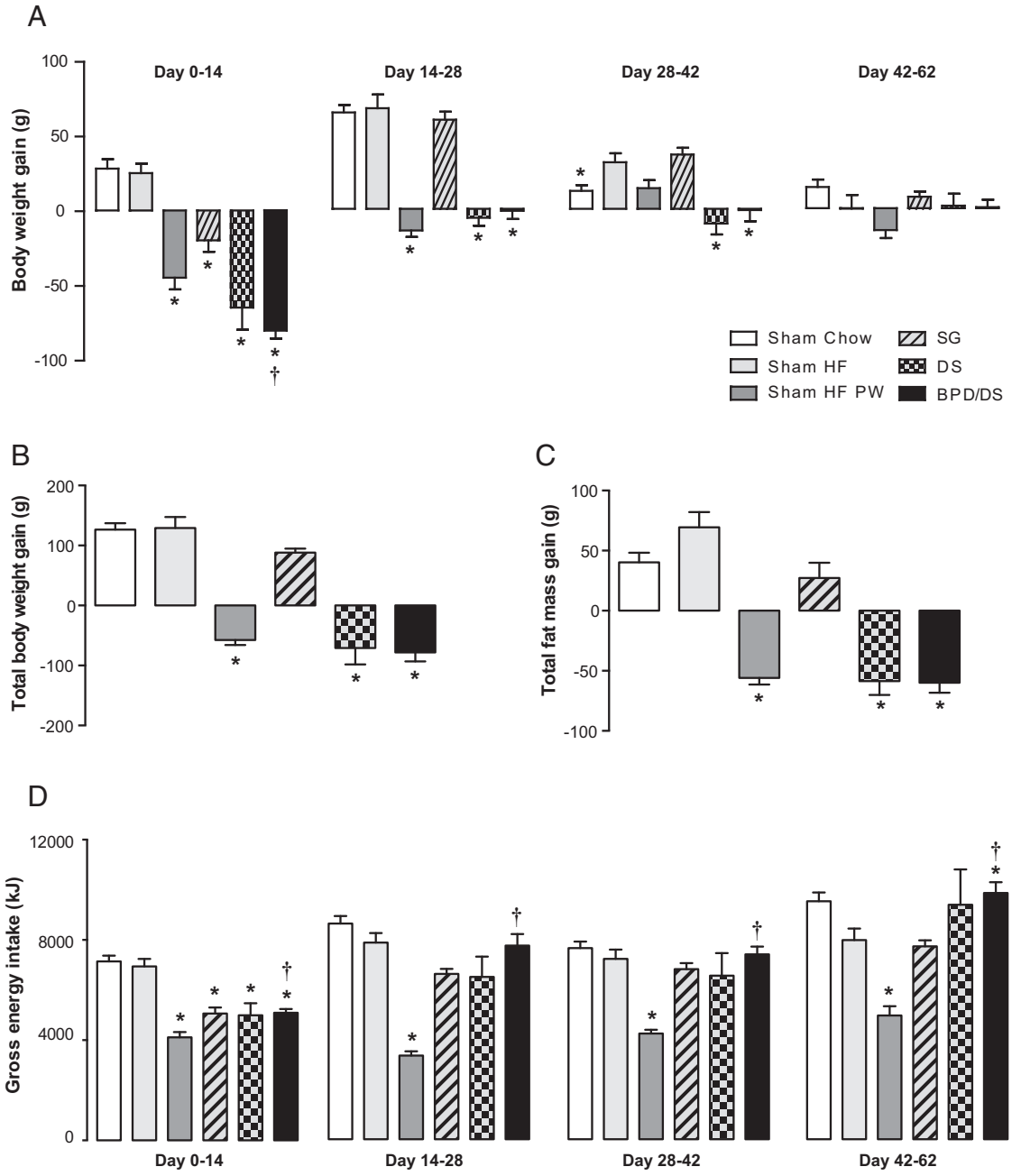

Figure 1. Effects of BPD, DS, SG, and sham operation on body weight, food intake, and body composition. Body weight gain (A) and gross energy intake (D) over each of four 2-week postoperative periods are shown. Body weight gain (B) and fat mass gain (C) at the end of 9 weeks after surgery also are shown. Data are means ± SEM. *, $P < .05$ vs sham HF; †, $P < .05$ for BPD vs sham HF PW.

sham-operated animals throughout the second part of the study (Figure 2A). Also, the amount of feces was greater in BPD/DS and DS rats. Consequently, fecal energy loss was significantly higher in BPD/DS and DS rats (Figure 2B). Even though gross energy intake was not significantly changed by bariatric surgery (Figure 2C), intestinal malabsorption led to a significant reduction in digestible energy intake in BPD/DS and DS rats during the second part of the experimental period (Figure 2D). Energy digestibility of the ingested food was accordingly reduced in BPD/DS and DS rats as compared with shams (Figure 2E). Fecal energy density in Sham HF rats was higher than in Sham Chow animals (Figure 2A). However, throughout the study, the Sham Chow rats had higher fecal excreta and higher fecal energy loss over 24 hours as compared with Sham HF rats (Figure 2B).

The meal intake test revealed that SG caused a persistent restriction. Six weeks after surgery, SG and BPD/DS rats consumed significantly less food during a meal than Sham HF animals (2.74 ± 0.24 g in SG and 3.06 ± 0.41 g

Table 1. Body Weight and Tissue Weights in BPD/DS, DS, SG, and Sham-Operated Rats at 9 Weeks Postoperatively

	Sham Chow	Sham HF	Sham HF PW	SG	DS	BPD/DS
Body weight, g	615.2 ± 20.5	648.4 ± 29.6	462.6 ± 16.9[a]	614.8 ± 19.3	462.0 ± 28.0[a]	460.2 ± 19.7[a]
iBAT, g	0.70 ± 0.05[a]	1.07 ± 0.08	0.40 ± 0.03[a]	0.85 ± 0.06[a]	0.33 ± 0.03[a]	0.37 ± 0.04[a]
Sum of WAT depots, g	44.44 ± 5.18[a]	69.67 ± 13.15	25.93 ± 1.75[a]	66.23 ± 3.37	20.21 ± 3.90[a]	20.66 ± 3.49[a]
Soleus muscle, g	0.315 ± 0.018[P = 0.06]	0.271 ± 0.018	0.272 ± 0.017	0.298 ± 0.009	0.245 ± 0.013	0.247 ± 0.012
EDL muscle, g	0.286 ± 0.013[a]	0.242 ± 0.008	0.239 ± 0.010	0.257 ± 0.009	0.197 ± 0.014[a]	0.204 ± 0.009[a,b]
Liver, g	17.47 ± 0.92	16.33 ± 0.58	10.27 ± 0.47[a]	14.78 ± 0.57	13.91 ± 0.91[a]	14.49 ± 0.64[a,b]
Pancreas, g	2.43 ± 0.09	2.03 ± 0.10	1.68 ± 0.11	2.18 ± 0.13	2.71 ± 0.25[a]	2.97 ± 0.16[a,b]
Heart, g	1.50 ± 0.05	1.49 ± 0.10	1.23 ± 0.05[a]	1.55 ± 0.06	1.21 ± 0.06[a]	1.28 ± 0.02[a]

Data were collected after a 16-hour fasting period. Data are means ± SEM.

[a] $P < .05$ vs sham HF.

[b] $P < .05$ for BPD/DS vs sham HF PW.

in BPD/DS vs 6.27 ± 0.82 g in Sham HF, $P < .05$, one-way ANOVA).

Gut morphology

Bariatric surgery resulted in changes in gut morphology (Figure 3). The mucosal layer was significantly thicker in the alimentary (Figure 3A) and common limbs (Figure 3B) in BPD/DS and DS rats compared with Sham HF. In contrast, SG and sham surgery did not affect the morphology of the proximal and distal ileum.

Energy expenditure and locomotor activity

The basal VO_2 measured over a 22-hour period was significantly lower in the BPD/DS, DS, and Sham HF PW rats compared with the Sham HF rats ($P < .05$, RM-ANOVA for comparing curve profiles, Figure 4A). No difference in this variable was observed between the SG and the sham-operated groups or between BPD/DS and DS animals. Sham HF PW rats even showed a lower VO_2 consumption than that of BPD/DS rats during the dark phase ($P < .05$, RM-ANOVA for comparing curve profiles, Figure 4A, and one-way ANOVA for areas under the curve, Figure 4B) but not during the light phase (Figure 4, A and C).

Basal RQ in the HF groups was lower than in chow-fed animals throughout the 22-hour experimental period (Figure 4D and dark and light phase averages, Figure 4, E and F). SG rats presented a RQ comparable with that of the Sham HF animals, suggesting that SG did not significantly affect substrate oxidation. During the dark phase, DS rats showed higher RQ than sham HF rats, reflecting an increase in carbohydrate oxidation (Figure 3D and dark phase averages, Figure 4E). A similar trend was observed in BPD/DS rats compared with Sham HF animals ($P = .07$, Figure 4E). During the dark phase, BPD/DS rats showed higher RQ than Sham HF PW animals (Figure 4E).

Locomotor activity (distance traveled) was affected by the different surgeries (Figure 4, G–I). Sham HF PW rats showed a significantly higher locomotor activity than the other groups, notwithstanding the phase of the day (Figure 4, G–I). During the dark phase, SG and Sham Chow rats also showed higher locomotor activity than Sham HF animals (Figure 4H). No difference was observed in the locomotor activity between the DS, BPD/DS, and Sham HF rats.

Thermogenic capacity and activity of iBAT

iBAT genes coding for UCP1 and proteins involved in fatty acid oxidation were modulated by the bariatric surgery treatments (Figure 5). In Sham HF there was a marked overexpression of CPT1 (Figure 5B) in parallel with trends toward increases in UCP1 and PGC1α mRNA expressions in iBAT (Figure 5, A and C). Chronic food deprivation induced a significant decrease in iBAT UCP1 and CPT1 mRNA along with a trend toward a reduction in PGC1α mRNA expression, suggesting a lower iBAT thermogenic in Sham HF PW rats compared with Sham HF rats ($P < .05$, Figure 5, A and B). The thermogenic capacity of iBAT seemed to be even more decreased in BPD/DS and DS groups, which showed reduced mRNA expressions of UCP1 (Figure 5A), CPT1 (Figure 5B), and COX4 (Figure 5D), compared with Sham HF. Noteworthily, SG rats exhibited an increase in PGC1α mRNA expression in BAT (Figure 5C). The two surgeries associated with body fat loss (BPD/DS and DS) showed a diminution of iBAT oxidative activity and iBAT fatty acid uptake (active iBAT volume) at 8 weeks after surgery (Figure 5, E–G). In contrast, SG resulted in a significant increase in active iBAT volume and iBAT oxidative metabolism (Figure 5, E–G).

GI hormones

BPD/DS and DS produced significant increases (vs Sham HF) in fasting plasma levels of GLP-1 and PYY

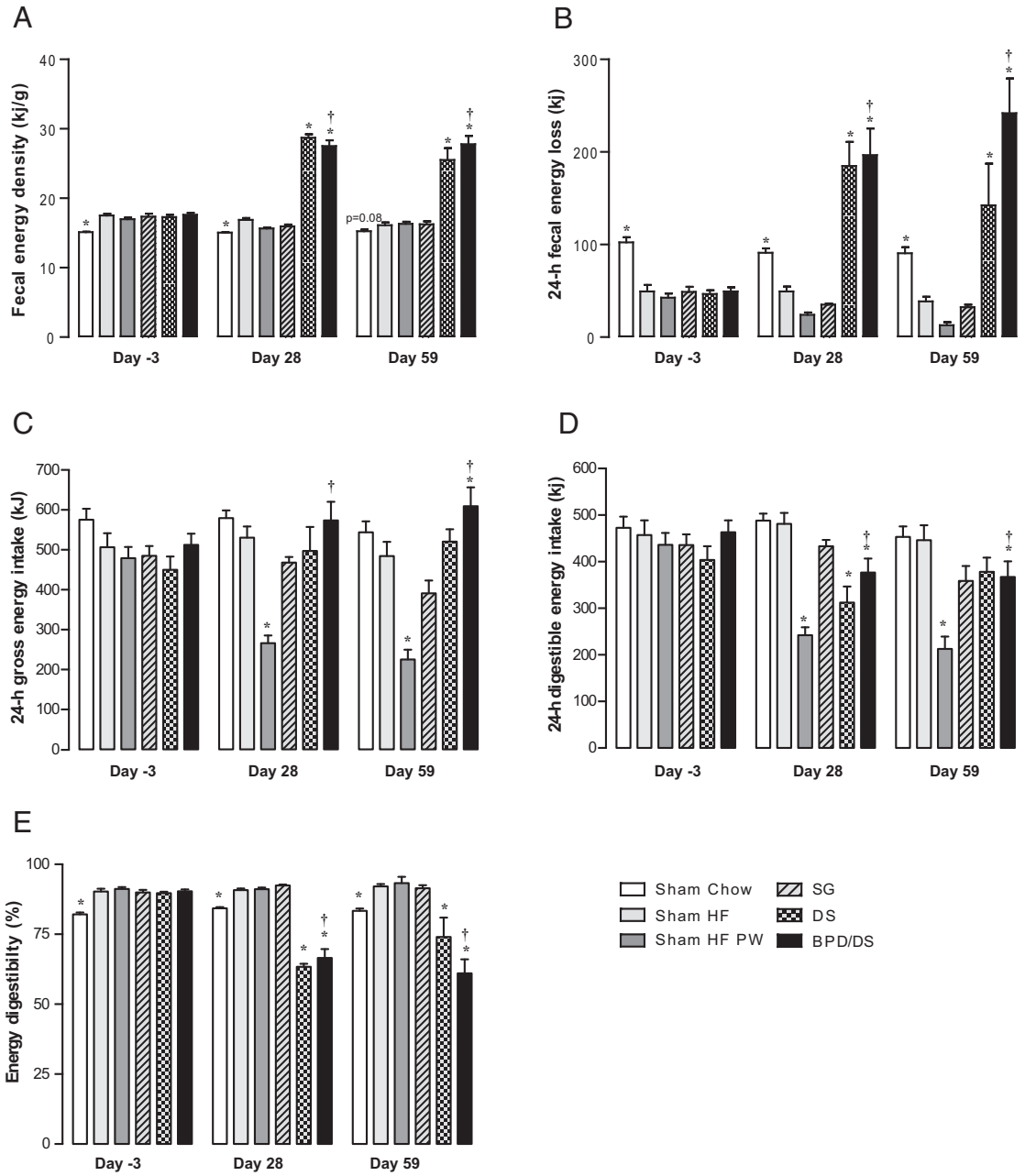

Figure 2. Effects of BPD, DS, SG, and sham operation on fecal energy density (A), fecal energy loss (B), gross energy intake (C), digestible energy intake (D) and energy digestibility (E). Measurements were taken over a 24-hour period prior to the surgery (day −3) and on postoperative days 28 and 59. Data are means ± SEM. *, $P < .05$ vs sham HF; †, $P < .05$ for BPD vs sham HF PW.

compared with the other groups (Figure 6, A and B). This effect was strongly associated with DS because no effect on plasma levels of these two gut hormones was observed after SG or sham operation. GIP plasma levels were also elevated in BPD/DS rats compared with Sham HF (Figure 6C). GLP-1, PYY, and GIP plasma levels were not affected by chronic food deprivation per se because no significant difference was observed between the Sham HF PW rats and the other sham-operated groups of animals (Figure 6, A–C). An increase in fasting acylated ghrelin was observed in Sham HF PW animals (Figure 6D). The HF-induced inhibitory effect (vs Sham Chow) on plasma levels of acylated ghrelin (Figure 6D) was reversed by the BPD/DS procedure (Figure 6D).

Glucose and lipid metabolism

As reflected by plasma insulin and C-peptide levels, the increase in insulin secretion in response to HF was maintained in Sham HF animals (vs Sham Chow) at 9 weeks after the surgery (Table 2). DS reversed this effect. At the time the animlas were killed, BPD/DS and DS animals showed levels of insulin and C-peptide similar to that of

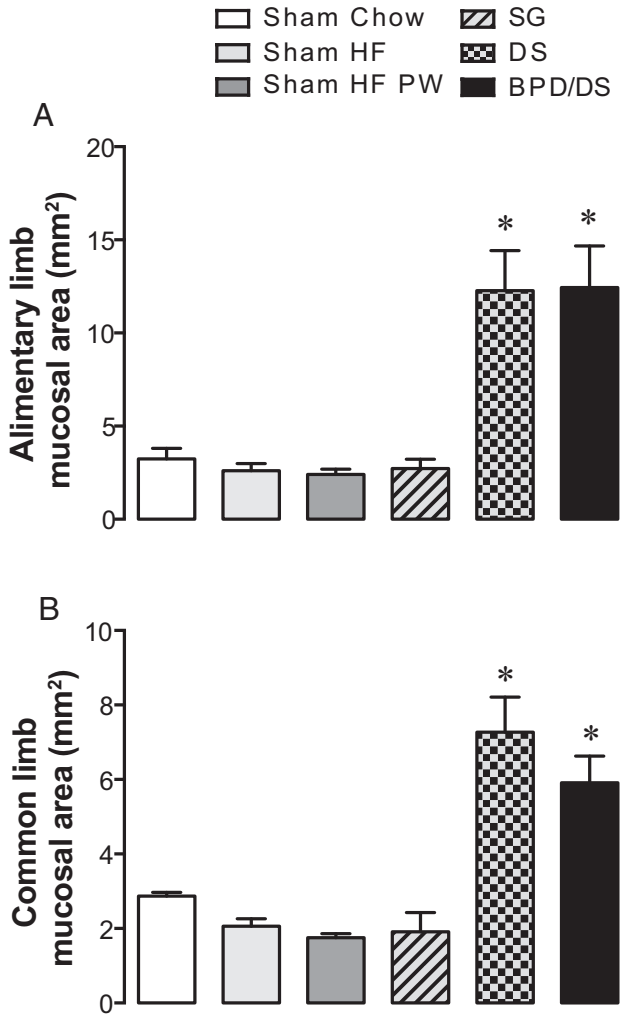

Figure 3. Effects of BPD, DS, SG, and sham operation on gut mucosal surface. Mucosal area of the alimentary (A) and common (B) limbs in BPD/DS and DS rats and proximal and distal ileum in SG and sham operated rats was measured on gut transversal sections. Data represent means ± SEM. *, $P < .05$ vs sham HF.

Sham Chow rats (Table 2). As reflected by the homeostasis model assessment index of insulin resistance index at 8 weeks after the surgery, BPD/DS and DS rats showed similar levels of insulin sensitivity to the Sham HF PW and Sham Chow animals (Supplemental Figure 4). Consistent with the body fat content, plasma leptin levels were lowered by BPD/DS, DS and food restriction at the levels of Sham Chow animals (Table 2). A slight reduction (vs Sham HF) in plasma leptin was also observed in SG rats (Table 2). At the time the animals were killed, no difference in plasma glucose, cholesterol, and NEFA levels was observed between groups. Regarding plasma triglycerides, only sham HF PW animals showed lower levels compared with the BPD/DS (Table 2).

Discussion

The present study was designed to assess the contribution of DS and SG to the metabolic and homeostatic effects of BPD/DS in HF-fed rats. BPD/DS and DS, but not SG, led to persistent reductions in body weight gain and body fat, which were accompanied by a significant decrease in digestible energy intake. BPD/DS and DS also exhibited a reduction in energy expenditure, which was largely but not totally accounted for by the reduction in body weight led to by the surgeries; energy expenditure was slightly higher in BPD/DS rats than in Sham HF PW animals. It is noteworthy that BPD/DS and DS reduced iBAT oxidative activity (estimated from ^{11}C-acetate) to the level seen in Sham HF PW. BPD/DS and DS led to significant elevations in GLP-1 and PYY levels. Altogether the present results emphasize the importance of the DS component of BPD/DS in creating a negative energy balance through reducing digestible energy intake. The DS component is unique to the BPD/DS and likely behind the established efficacy of the procedure to treat obesity and resolve type 2 diabetes (38, 39). The significance of DS was recently acknowledged by Pata et al (40), who demonstrated that a bariatric intervention, which consisted of a permanent DS and transient (for 6–8 mo) gastroplasty, could produce a reduced body mass index after 10–15 years. A recent report from our group also emphasized the importance of the DS component in humans, in particular on the long-term effects of the surgery (41).

The present results demonstrate that BPD/DS and DS create a negative energy balance through reducing the digestibility of food. Digestible energy intake was indeed lower in BPD/DS and DS rats than in Sham HF animals. The observation that BPD/DS rats ate more than Sham HF PW animals to maintain the same body weight and fat mass demonstrates the ability of BPD/DS to also stimulate energy expenditure. In line with this, dark-phase VO_2 and RQ were in fact higher in BPD/DS than in Sham HF PW. However, BPD/DS did not apparently sustain energy expenditure through increasing iBAT thermogenesis. iBAT thermogenic activity determined with ^{11}C-acetate, and free fatty acid uptake measured with ^{18}FTHA, were noticeably reduced in BPD/DS rats. Consonantly, levels of expression of iBAT genes encoding UCP1, CPT1b, and COX4 in BPD/DS and DS rats were below those of Sham HF PW rats. Other investigators (42) have similarly denied the role of BAT in the increase in energy expenditure led to by RYGB. BAT is a heat-producing tissue whose activity is mainly controlled by the sympathetic nervous system (43), and RYGB has been demonstrated to reduce sympathetic nervous system activity (44). The mechanisms whereby BPD/DS stimulated energy expenditure while reducing BAT thermogenesis remain to be determined. They are apparently related to the DS component as SG alone neither changed expenditure nor reduced energy expenditure in the present study. The DS-mediated increase in

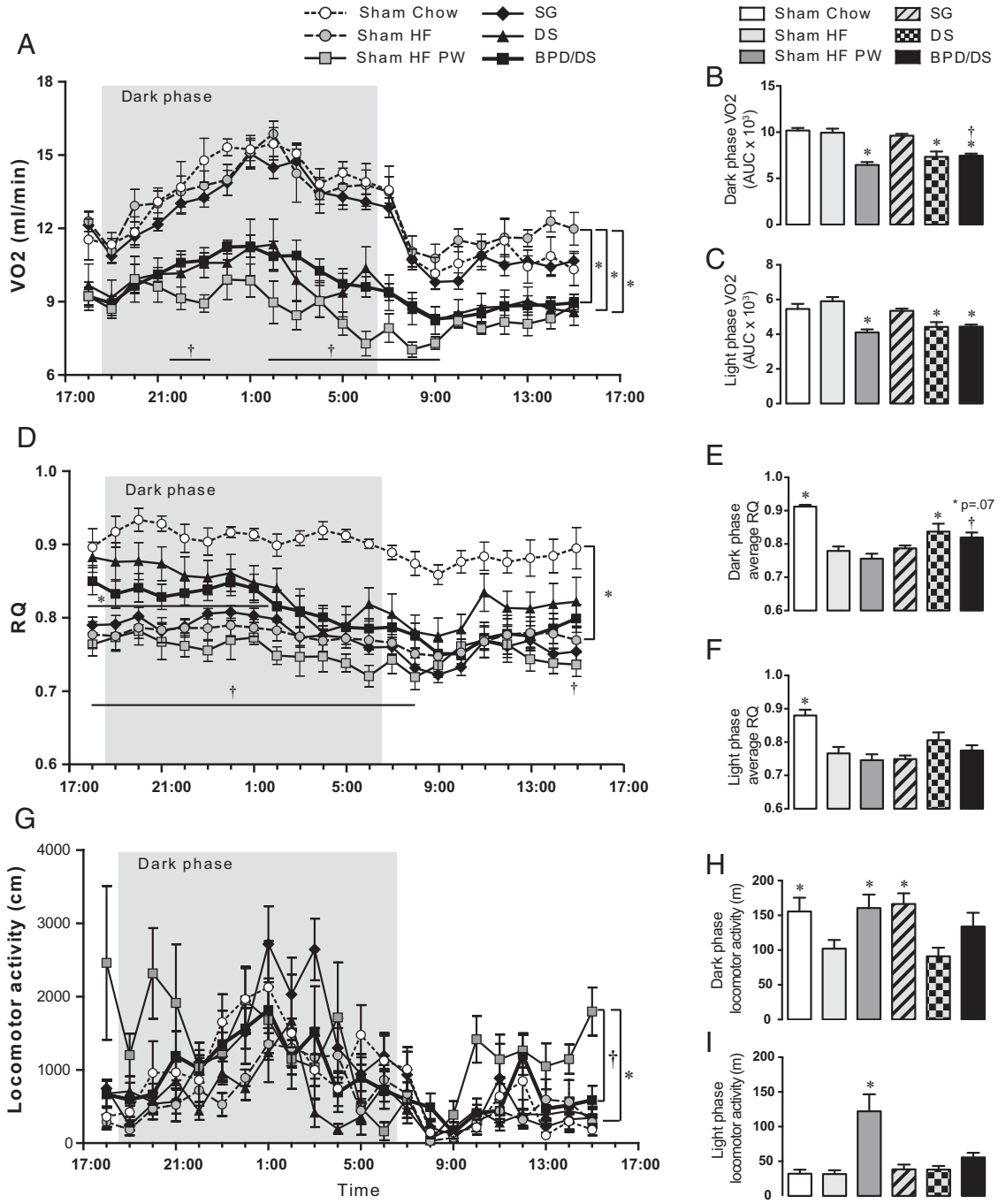

Figure 4. Effects of BPD, DS, SG, and sham operation on basal energy expenditure. VO_2, RQ, and locomotor activity were measured every 15 minutes over a 22-hour dark/light period at 8 weeks postoperatively. VO_2 is presented as hourly averages of measurements taken over a 22-hour period (A) and areas under the curve (AUC) obtained during the dark (B) and light phase (C). RQ is presented as hourly averages of measurements taken over the 22-hour period (D) and averages of values obtained during the dark (E) and light phase (F). Locomotor activity is presented as hourly averages over the 22-hour period (G) and total distance traveled during the dark (H) and light phase (I). Data are means ± SEM. *, $P < .05$ vs sham HF; †, $P < .05$ for BPD vs sham HF PW.

BPD/DS-induced GLP-1 and PYY does not appear as a likely mechanism because the elevation of these GI hormones is more stimulatory than inhibitory on BAT thermogenesis (45, 46).

One aspect that deserves consideration in explaining the increase in metabolic rate and the decrease in iBAT activity/capacity in BPD/DS compared with Sham HF PW is the effect of the surgery on the morphology of the intestine. One can arguably predict that an increase in gut wall thickness in both the alimentary and common limbs can increase the capacity of the intestine to produce heat and consequently to suppress iBAT activity. This hypoth-

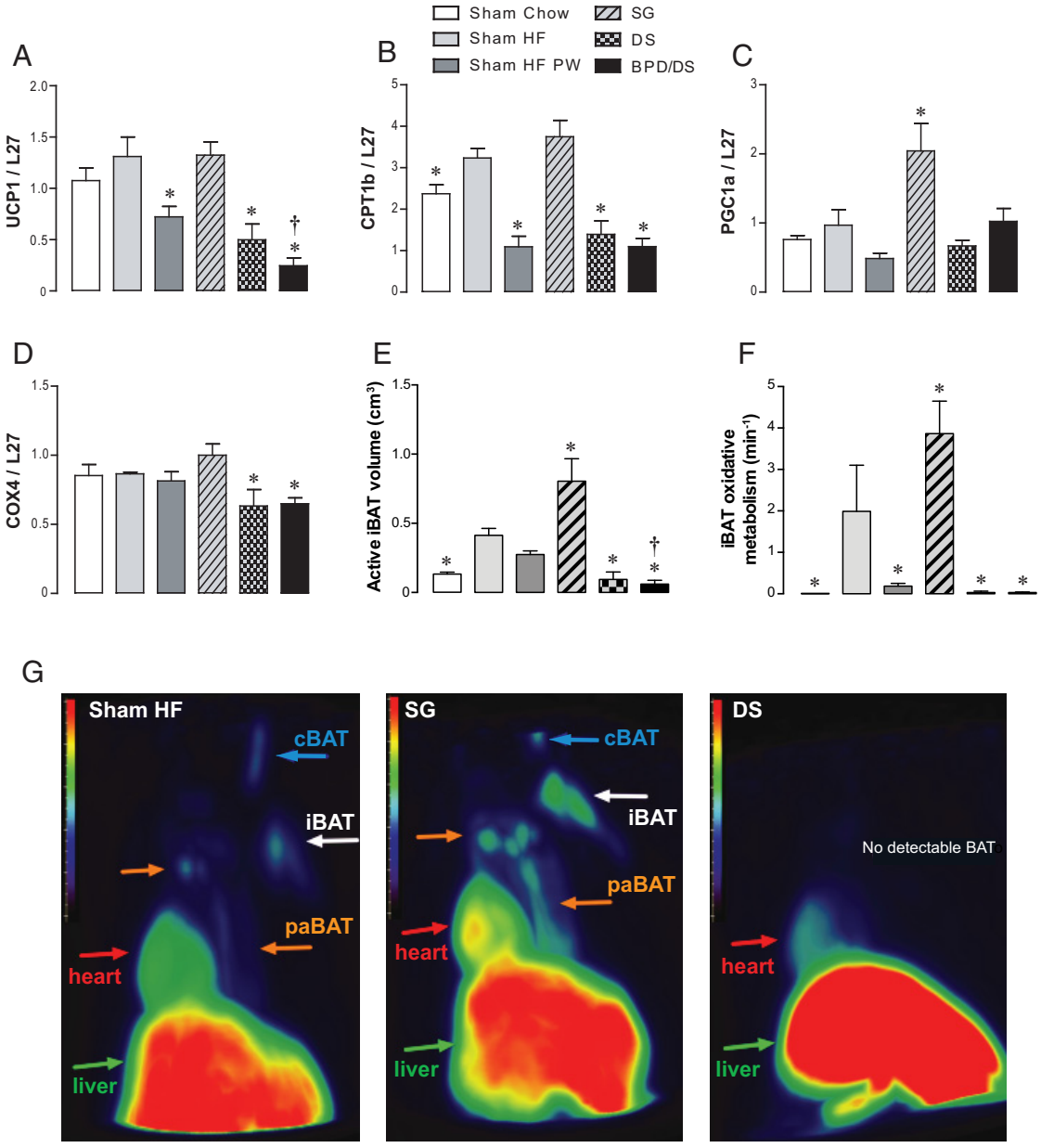

Figure 5. Effects of BPD, DS, SG, and sham operation on iBAT thermogenetic capacity and activity. Levels of mRNA expression of UCP1 (A), CPT1b (B), PGC1α (C), and COX4 (D) were measured in iBAT at 9 weeks, postoperatively. Active iBAT volume (E and G) and oxidative metabolism (F) were determined after a dynamic acquisition of ^{18}FTHA and [^{11}C]acetate, respectively. Imaging experiments were performed at 8 weeks postoperatively. Data are means ± SEM. iBAT, interscapular BAT; cBAT, cervical BAT; paBAT, periaortic BAT. *, $P < .05$ vs sham HF; †, $P < .05$ for BPD vs sham HF PW.

esis, however, needs to be verified. The gut is a very metabolically active tissue that accounts for 15%–22% total oxygen consumption (42).

SG alone resulted in a transient reduction in food intake and delayed body weight gain, but it did not significantly altered body composition on the long term. These results are consistent with our previous data from a study conducted in chow-fed animals (9), but they contrast with results obtained in rats by other investigators who demonstrated weight reduction, even after 2 years following (47). The body weight reducing effect seems to be related to the amount of the stomach tissue that is removed in the SG (48). For instance, Stefater et al (49) excised 80% of the stomach, whereas we removed approximately 60% of the organ. Our results nonetheless indicate that SG exerts a reducing acute effect on meal intake but did not prevent HF-induced excess weight gain in the long term in rats. In this study as well as in our preceding one carried out in chow-fed rats, SG rats appeared capable to compensate the restricting effects of the gastrectomy. In terms of practicability, SG has certainly advantages over BPD/DS, and it has proved to be effective at inducing weight loss in

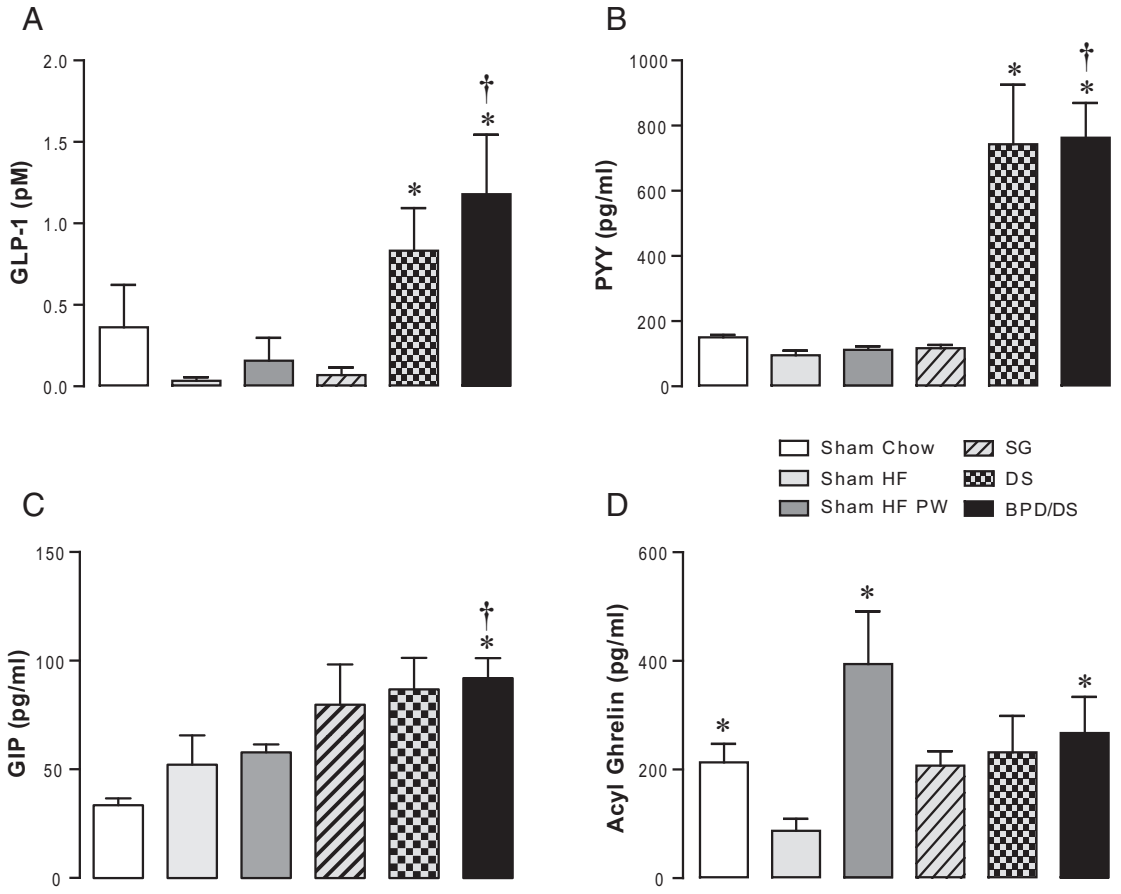

Figure 6. Effects of BPD, DS, SG, and sham-operation on basal secretion of GI hormones. Plasma levels of GLP-1_{3-36} (A), PYY (B), GIP (C), and acylated ghrelin (D) were measured at 9 weeks postoperatively. Data are means ± SEM. *, $P < .05$ vs sham HF; †, $P < .05$ for BPD vs sham HF PW.

humans (50) and even has been described as the ideal weight-loss surgery (51). Additionally, SG has been successfully used as a first stage of the BPD/DS procedure in severely obese people, in whom it reduces body weight and thereby facilitates the derivation step of the BPD/DS (52). However, whether SG can produce in humans long-lasting effect (>5 y) on body weight still needs to be substantiated (53). Although this work was in progress, it was reported by Marceau et al that SG patients regain weight much faster than those with DS (41).

BPD/DS and DS resulted in increased plasma levels of the gut hormones GLP-1 and PYY. Elevations of GLP-1 and PYY have been previously observed in human (54–57) and animal (58, 59) studies after bariatric surgery. GLP-1 and PYY are satiating hormones cosecreted by the intestinal L cells located in the distal gut (60–62). After the

Table 2. Plasma Metabolites and Hormones in BPD/DS, DS, SG, and Sham-Operated Rats at 9 Weeks Postoperatively

	Sham Chow	Sham HF	Sham HF PW	SG	DS	BPD/DS
Glucose, mM	9.85 ± 0.60	9.51 ± 0.82	9.34 ± 0.41	9.59 ± 0.67	8.37 ± 0.70	7.77 ± 0.38
Insulin, pM	67.29 ± 3.23[a]	98.52 ± 13.10	61.52 ± 3.12[a]	96.21 ± 7.63	56.50 ± 2.33[a]	63.90 ± 5.90[a]
C-peptide, nM	0.49 ± 0.05[a]	1.05 ± 0.15	0.30 ± 0.04[a]	0.75 ± 0.07	0.25 ± 0.06[a]	0.27 ± 0.05[a]
Leptin, μg/mL	0.71 ± 0.01[a]	2.18 ± 0.60	0.32 ± 0.05[a]	1.12 ± 0.09[a]	0.20 ± 0.05[a]	0.27 ± 0.08[a]
Cholesterol, mM	4.01 ± 0.34	3.68 ± 0.42	3.10 ± 0.35	3.07 ± 0.29	3.21 ± 0.51	2.77 ± 0.32
Triglycerides, mM	0.49 ± 0.06	0.48 ± 0.06	0.24 ± 0.03	0.37 ± 0.04	0.48 ± 0.06	0.50 ± 0.07[b]
NEFA, mM	0.39 ± 0.05	0.32 ± 0.01	0.33 ± 0.04	0.31 ± 0.03	0.32 ± 0.04	0.39 ± 0.04

Data were collected after a 16-hour fasting period. Data represent means ± SEM.

[a] $P < .05$ vs sham HF ad libitum.

[b] $P < .05$ for BPD vs sham HF PW.

upper intestine bypass, the distal ileum receives nutrients partially digested and a consequent hypertrophy of the mucosa is developing to increase nutriment absorption. Confirming previous data (10), we observed in this study that BPD/DS and DS resulted in a notable hypertrophy of the alimentary and common limbs. The mucosal hypertrophy of the gut leads to a significant increase in L cell number and gut capacity to secrete more GLP-1 and PYY (9). Our three bariatric procedures led to an increase in GIP plasma levels. GIP is an incretin secreted by the duodenal and jejunal K cells in response to partially digested nutrients in the intestinal lumen. There is still inconsistency in data reported on GIP levels after bariatric surgery. Studies in humans have reported decrease or no change in GIP secretion after BPD or RYGB (63–67). In contrast, animal studies have shown increases in GIP after bariatric procedures involving duodenum or jejunum bypass (68, 69). Our models of BPD/DS and DS with the exclusion of the foregut from the alimentary tract resulted in an increase in GIP secretion. It was suggested that the presence of partially digested nutrients stimulate the synthesis of GIP in the enteroendocrine cells from the distal gut (68). It was demonstrated that intestinal GIP protein content is increased in the midjejunum and the common channel after duodeno-jejunal bypass in rats, whereas no change was observed in the duodenal GIP content in the bypassed segment (68). However, for a better understanding of gut hormones physiology after bariatric procedures, an assessment should have been done in both fasted and after food ingestion.

Discrepant results have also been reported regarding changes in plasma ghrelin after bariatric surgery. We observed that HF feeding induced an inhibitory effect on fasting levels of acylated ghrelin, which is consistent with the data showing that long-term intake of a HF diet results in hypoghrelinemia (70). This effect was reversed by bariatric surgery, particularly by BPD/DS. After SG, we did not observed the decrease in fasting ghrelin levels observed by others (71). Again, it is noteworthy that in our model, SG consisted in the removal of the aglandular forestomach and the remnant sleeve keeps almost intact the pool of ghrelin secreting cells. It is also worth mentioning the persistence of the appetite-stimulating hormone ghrelin did not compensate for the negative energy balance induced by intestinal malabsorption.

In summary, the present study indicates that the DS component of the BPD/DS surgery is a major contributor to the long-term effects of BPD/DS on energy balance in diet-induced obese rats. The DS component leads to a reduction in digestible energy intake while sustaining energy expenditure. The intestinal diversion by DS also results in gut morphological changes, which are accompanied by elevation in satiating gut hormones such as GLP-1 and PYY.

Acknowledgments

We thank Cynthia Bouchard, Audrey Chalifoux, and Samuel Dubé for their animal care help and Julie Plamondon and Yves Gelinas for technical assistance.

Address all correspondence and requests for reprints to: Denis Richard, PhD, Direction de la Recherche, Québec Heart and Lung Institute, 2725, Chemin Sainte-Foy, Québec, Canada G1V 4G5. E-mail: denis.richard@criucpq.ulaval.ca.

This work was supported by the Laval University Research Chair on Obesity.

Disclosure Summary: The authors have nothing to disclose.

References

1. **Biertho L, Biron S, Hould FS, Lebel S, Marceau S, Marceau P.** Is biliopancreatic diversion with duodenal switch indicated for patients with body mass index <50 kg/m^2? *Surg Obes Relat Dis*. 2010; 6(5):508–514.
2. **Biron S, Hould FS, Lebel S, et al.** Twenty years of biliopancreatic diversion: what is the goal of the surgery? *Obes Surg*. 2004;14(2): 160–164.
3. **Marceau P, Hould FS, Potvin M, Lebel S, Biron S.** Biliopancreatic diversion (doudenal switch procedure). *Eur J Gastroenterol Hepatol*. 1999;11(2):99–103.
4. **Buchwald H, Oien DM.** Metabolic/bariatric surgery worldwide, 2011. *Obes Surg*. 2013;23(4):427–436.
5. **Moustarah F, Gilbert A, Despres JP, Tchernof A.** Impact of gastrointestinal surgery on cardiometabolic risk. *Curr Atheroscler Rep*. 2012;14(6):588–596.
6. **Colquitt JL, Pickett K, Loveman E, Frampton GK.** Surgery for weight loss in adults. *Cochrane Database Syst Rev*. 2014: CD003641.
7. **Yu J, Zhou X, Li L, et al.** The long-term effects of bariatric surgery for type 2 diabetes: systematic review and meta-analysis of randomized and non-randomized evidence. *Obes Surg*. 2015;25(1):143–158.
8. **Marceau P, Biron S, Bourque RA, Potvin M, Hould FS, Simard S.** Biliopancreatic diversion with a new type of gastrectomy. *Obes Surg*. 1993;3(1):29–35.
9. **Li W, Baraboi ED, Cluny NL, et al.** Malabsorption plays a major role in the effects of the biliopancreatic diversion with duodenal switch on energy metabolism in rats. *Surg Obes Relat Dis*. Published online August 12, 2014. DOI: 10.1016/j.soard.2014.07.020
10. **Nadreau E, Baraboi ED, Samson P, et al.** Effects of the biliopancreatic diversion on energy balance in the rat. *Int J Obes (Lond)*. 2006; 30(3):419–429.
11. **Adami GF, Campostano A, Gandolfo P, Marinari G, Bessarione D, Scopinaro N.** Body composition and energy expenditure in obese patients prior to and following biliopancreatic diversion for obesity. *Eur Surg Res*. 1996;28(4):295–298.
12. **Greenway FL.** Surgery for obesity. *Endocrinol Metab Clin North Am*. 1996;25(4):1005–1027.
13. **Bueter M, Lowenstein C, Olbers T, et al.** Gastric bypass increases energy expenditure in rats. *Gastroenterology*. 2010;138(5):1845–1853.
14. **Flancbaum L, Choban PS, Bradley LR, Burge JC.** Changes in mea-

sured resting energy expenditure after Roux-en-Y gastric bypass for clinically severe obesity. *Surgery*. 1997;122(5):943–949.
15. **Stylopoulos N, Hoppin AG, Kaplan LM.** Roux-en-Y gastric bypass enhances energy expenditure and extends lifespan in diet-induced obese rats. *Obesity*. 2009;17(10):1839–1847.
16. **Werling M, Olbers T, Fandriks L, et al.** Increased postprandial energy expenditure may explain superior long term weight loss after Roux-en-Y gastric bypass compared to vertical banded gastroplasty. *PLoS One*. 2013;8(4):e60280.
17. **Carrasco F, Papapietro K, Csendes A, et al.** Changes in resting energy expenditure and body composition after weight loss following Roux-en-Y gastric bypass. *Obes Surg*. 2007;17(5):608–616.
18. **Das SK, Roberts SB, McCrory MA, et al.** Long-term changes in energy expenditure and body composition after massive weight loss induced by gastric bypass surgery. *Am J Clin Nutr*. 2003;78(1):22–30.
19. **Zheng H, Shin AC, Lenard NR, et al.** Meal patterns, satiety, and food choice in a rat model of Roux-en-Y gastric bypass surgery. *Am J Physiol Regul Integr Comp Physiol*. 2009;297(5):R1273–R1282.
20. **Le Roux CW, Bueter M, Theis N, et al.** Gastric bypass reduces fat intake and preference. *Am J Physiol Regul Integr Comp Physiol*. 2011;301(4):R1057–R1066.
21. **Wilson-Perez HE, Chambers AP, Sandoval DA, et al.** The effect of vertical sleeve gastrectomy on food choice in rats. *Int J Obes (Lond)*. 2013;37(2):288–295.
22. **Braghetto I, Davanzo C, Korn O, et al.** Scintigraphic evaluation of gastric emptying in obese patients submitted to sleeve gastrectomy compared to normal subjects. *Obes Surg*. 2009;19(11):1515–1521.
23. **Shah S, Shah P, Todkar J, Gagner M, Sonar S, Solav S.** Prospective controlled study of effect of laparoscopic sleeve gastrectomy on small bowel transit time and gastric emptying half-time in morbidly obese patients with type 2 diabetes mellitus. *Surg Obes Relat Dis*. 2010;6(2):152–157.
24. **Naslund I, Beckman KW.** Gastric emptying rate after gastric bypass and gastroplasty. *Scand J Gastroenterol*. 1987;22(2):193–201.
25. **Suzuki S, Ramos EJ, Goncalves CG, Chen C, Meguid MM.** Changes in GI hormones and their effect on gastric emptying and transit times after Roux-en-Y gastric bypass in rat model. *Surgery*. 2005;138(2):283–290.
26. **Chambers AP, Smith EP, Begg DP, et al.** Regulation of gastric emptying rate and its role in nutrient-induced GLP-1 secretion in rats after vertical sleeve gastrectomy. *Am J Physiol Endocrinol Metab*. 2014;306(4):E424–E432.
27. **Korner J, Bessler M, Cirilo LJ, et al.** Effects of Roux-en-Y gastric bypass surgery on fasting and postprandial concentrations of plasma ghrelin, peptide YY, and insulin. *J Clin Endocrinol Metab*. 2005;90(1):359–365.
28. **le Roux CW, Aylwin SJ, Batterham RL, et al.** Gut hormone profiles following bariatric surgery favor an anorectic state, facilitate weight loss, and improve metabolic parameters. *Ann Surg*. 2006;243(1):108–114.
29. **Clements RH, Gonzalez QH, Long CI, Wittert G, Laws HL.** Hormonal changes after Roux-en Y gastric bypass for morbid obesity and the control of type II diabetes mellitus. *Am Surg*. 2004;70(1):1–4; discussion 4–5.
30. **Cummings BP, Bettaieb A, Graham JL, et al.** Vertical sleeve gastrectomy improves glucose and lipid metabolism and delays diabetes onset in UCD-T2DM rats. *Endocrinology*. 2012;153(8):3620–3632.
31. **Sweeney TE, Morton JM.** The human gut microbiome: a review of the effect of obesity and surgically induced weight loss. *JAMA Surg*. 2013;148(6):563–569.
32. **Ryan KK, Tremaroli V, Clemmensen C, et al.** FXR is a molecular target for the effects of vertical sleeve gastrectomy. *Nature*. 2014;509(7499):183–188.
33. **Marceau P, Hould FS, Simard S, et al.** Biliopancreatic diversion with duodenal switch. *World J Surg*. 1998;22(9):947–954.
34. **Menard SL, Croteau E, Sarrhini O, et al.** Abnormal in vivo myocardial energy substrate uptake in diet-induced type 2 diabetic cardiomyopathy in rats. *Am J Physiol Endocrinol Metab*. 2010;298(5):E1049–E1057.
35. **Ouellet V, Labbe SM, Blondin DP, et al.** Brown adipose tissue oxidative metabolism contributes to energy expenditure during acute cold exposure in humans. *J Clin Invest*. 2012;122(2):545–552.
36. **Bessi VL, Labbe SM, Huynh DN, et al.** EP 80317, a selective CD36 ligand, shows cardioprotective effects against post-ischaemic myocardial damage in mice. *Cardiovasc Res*. 2012;96(1):99–108.
37. **Labbe SM, Grenier-Larouche T, Croteau E, et al.** Organ-specific dietary fatty acid uptake in humans using positron emission tomography coupled to computed tomography. *Am J Physiol Endocrinol Metab*. 2011;300(3):E445–E453.
38. **Dorman RB, Rasmus NF, al-Haddad BJ, et al.** Benefits and complications of the duodenal switch/biliopancreatic diversion compared to the Roux-en-Y gastric bypass. *Surgery*. 2012;152(4):758–765; discussion 765–757.
39. **Rubino F, Schauer PR, Kaplan LM, Cummings DE.** Metabolic surgery to treat type 2 diabetes: clinical outcomes and mechanisms of action. *Annu Rev Med*. 2010;61:393–411.
40. **Pata G, Crea N, Di Betta E, Bruni O, Vassallo C, Mittempergher F.** Biliopancreatic diversion with transient gastroplasty and duodenal switch: Long-term results of a multicentric study. *Surgery*. 2013;153(3):413–422.
41. **Marceau P, Biron S, Marceau S, et al.** Biliopancreatic diversion-duodenal switch: independent contributions of sleeve resection and duodenal exclusion. *Obes Surg*. 2014;24(11):1843–1849.
42. **Cant JP, McBride BW, Croom WJ Jr.** The regulation of intestinal metabolism and its impact on whole animal energetics. *J Anim Sci*. 1996;74(10):2541–2553.
43. **Richard D, Monge-Roffarello B, Chechi K, Labbe SM, Turcotte EE.** Control and physiological determinants of sympathetically mediated brown adipose tissue thermogenesis. *Front Endocrinol (Lausanne)*. 2012;3:36.
44. **Curry TB, Somaraju M, Hines CN, et al.** Sympathetic support of energy expenditure and sympathetic nervous system activity after gastric bypass surgery. *Obesity*. 2013;21(3):480–485.
45. **Beiroa D, Imbernon M, Gallego R, et al.** GLP-1 agonism stimulates brown adipose tissue thermogenesis and browning through hypothalamic AMPK. *Diabetes*. 2014;63(10):3346–3358.
46. **Irwin N, Francis JM, Flatt PR.** Alterations of glucose-dependent insulinotropic polypeptide (GIP) during cold acclimation. *Regul Pept*. 2011;167(1):91–96.
47. **Stefater MA, Perez-Tilve D, Chambers AP, et al.** Sleeve gastrectomy induces loss of weight and fat mass in obese rats, but does not affect leptin sensitivity. *Gastroenterology*. 2010;138(7):2426–2436, 2436.e2421–2423.
48. **Langer FB, Reza Hoda MA, Bohdjalian A, et al.** Sleeve gastrectomy and gastric banding: effects on plasma ghrelin levels. *Obes Surg*. 2005;15(7):1024–1029.
49. **Stefater MA, Sandoval DA, Chambers AP, et al.** Sleeve gastrectomy in rats improves postprandial lipid clearance by reducing intestinal triglyceride secretion. *Gastroenterology*. 2011;141(3):939–949.e931–934.
50. **Fischer L, Hildebrandt C, Bruckner T, et al.** Excessive weight loss after sleeve gastrectomy: a systematic review. *Obes Surg*. 2012;22(5):721–731.
51. **Gagner M.** Sleeve gastrectomy: an ideal choice for T2DM. *Nat Rev Endocrinol*. 2013;9(10):623.
52. **Silecchia G, Boru C, Pecchia A, et al.** Effectiveness of laparoscopic sleeve gastrectomy (first stage of biliopancreatic diversion with duodenal switch) on co-morbidities in super-obese high-risk patients. *Obes Surg*. 2006;16(9):1138–1144.
53. **Puzziferri N, Roshek TB 3rd, Mayo HG, Gallagher R, Belle SH, Livingston EH.** Long-term follow-up after bariatric surgery: a systematic review. *JAMA*. 2014;312(9):934–942.

54. **Tsoli M, Chronaiou A, Kehagias I, Kalfarentzos F, Alexandrides TK.** Hormone changes and diabetes resolution after biliopancreatic diversion and laparoscopic sleeve gastrectomy: a comparative prospective study. *Surg Obes Relat Dis*. 2013;9(5):667–677.
55. **Werling M, Vincent RP, Cross GF, et al.** Enhanced fasting and postprandial plasma bile acid responses after Roux-en-Y gastric bypass surgery. *Scand J Gastroenterol*. 2013;48(11):1257–1264.
56. **Dar MS, Chapman WH 3rd, Pender JR, et al.** GLP-1 response to a mixed meal: what happens 10 years after Roux-en-Y gastric bypass (RYGB)? *Obes Surg*. 2012;22(7):1077–1083.
57. **Papamargaritis D, le Roux CW, Sioka E, Koukoulis G, Tzovaras G, Zacharoulis D.** Changes in gut hormone profile and glucose homeostasis after laparoscopic sleeve gastrectomy. *Surg Obes Relat Dis*. 2013;9(2):192–201.
58. **Borg CM, le Roux CW, Ghatei MA, Bloom SR, Patel AG.** Biliopancreatic diversion in rats is associated with intestinal hypertrophy and with increased GLP-1, GLP-2 and PYY levels. *Obes Surg*. 2007; 17(9):1193–1198.
59. **Kampe J, Stefanidis A, Lockie SH, et al.** Neural and humoral changes associated with the adjustable gastric band: insights from a rodent model. *Int J Obes (Lond)*. 2012;36(11):1403–1411.
60. **Bottcher G, Sjolund K, Ekblad E, Hakanson R, Schwartz TW, Sundler F.** Coexistence of peptide YY and glicentin immunoreactivity in endocrine cells of the gut. *Regul Pept*. 1984;8(4):261–266.
61. **Habib AM, Richards P, Rogers GJ, Reimann F, Gribble FM.** Co-localisation and secretion of glucagon-like peptide 1 and peptide YY from primary cultured human L cells. *Diabetologia*. 2013;56(6): 1413–1416.
62. **Wettergren A, Petersen H, Orskov C, Christiansen J, Sheikh SP, Holst JJ.** Glucagon-like peptide-1 7–36 amide and peptide YY from the L-cell of the ileal mucosa are potent inhibitors of vagally induced gastric acid secretion in man. *Scand J Gastroenterol*. 1994;29(6): 501–505.
63. **Guidone C, Manco M, Valera-Mora E, et al.** Mechanisms of recovery from type 2 diabetes after malabsorptive bariatric surgery. *Diabetes*. 2006;55(7):2025–2031.
64. **Jorgensen NB, Jacobsen SH, Dirksen C, et al.** Acute and long-term effects of Roux-en-Y gastric bypass on glucose metabolism in subjects with type 2 diabetes and normal glucose tolerance. *Am J Physiol Endocrinol Metab*. 2012;303(1):E122–E131.
65. **Mingrone G, Nolfe G, Gissey GC, et al.** Circadian rhythms of GIP and GLP1 in glucose-tolerant and in type 2 diabetic patients after biliopancreatic diversion. *Diabetologia*. 2009;52(5):873–881.
66. **Rubino F, Gagner M, Gentileschi P, et al.** The early effect of the Roux-en-Y gastric bypass on hormones involved in body weight regulation and glucose metabolism. *Ann Surg*. 2004;240(2):236–242.
67. **Salinari S, Bertuzzi A, Asnaghi S, Guidone C, Manco M, Mingrone G.** First-phase insulin secretion restoration and differential response to glucose load depending on the route of administration in type 2 diabetic subjects after bariatric surgery. *Diabetes Care*. 2009;32(3): 375–380.
68. **Kindel TL, Yoder SM, D'Alessio DA, Tso P.** The effect of duodenal-jejunal bypass on glucose-dependent insulinotropic polypeptide secretion in Wistar rats. *Obes Surg*. 2010;20(6):768–775.
69. **Rubino F, Marescaux J.** Effect of duodenal-jejunal exclusion in a non-obese animal model of type 2 diabetes: a new perspective for an old disease. *Ann Surg*. 2004;239(1):1–11.
70. **Gomez G, Han S, Englander EW, Greeley GH Jr.** Influence of a long-term high-fat diet on ghrelin secretion and ghrelin-induced food intake in rats. *Regul Pept*. 2012;173(1–3):60–63.
71. **Chambers AP, Kirchner H, Wilson-Perez HE, et al.** The effects of vertical sleeve gastrectomy in rodents are ghrelin independent. *Gastroenterology*. 2013;144(1):50–52.e55.